PAPER

Cite this: DOI: 10.1039/xxxxxxxxxx

Design & Performance of Mesofluidic diodes fabricated via multi-jet additive manufacturing†

V. Padia, J. Hardies, M. Martin, R. Poluhovich, and J. Singh

Received 14th December 2016

DOI: 1738./2016

www.rsc.org/

The design and implementation of mesofluidic valves presents students the opportunity to apply advanced additive manufacturing knowledge towards the complex processes involved with microfluidics. Here we examine the design process and performance of six valve designs printed with multi-jet modeling technology. The ultimate goal of the design challenge is to create a microfluidic diode that experimentally shows the largest Diodicity - the ratio of 'allowed' to 'obstructed' fluid flow.

1 Introduction

Additive manufacturing is an increasingly more versatile technology in the scientific community. Advancements in specific technologies such as multi-jet printing, has allowed users to consistently, accurately and iteratively print at the meso- and microscales for a multitude of applications. Additive manufacturing, or 3-D printing, has created applications in the biomedical field through applications including auto-titration, cellular culture analysis, and microfluidics. These direct applications have created an extensive field of research in the field of additive manufacturing.

Microfluidics has created opportunities for improved chemical applications such as drug screening and molecular diagnostics.[1] An understanding of the limitations and necessary design changes of each microfluidic component is vital to design useful microfluidic circuits. New technology capabilities in additive manufacturing has started to replace traditional microfluidic manufacturing techniques such as soft lithography.

Here, we investigated the design, manufacturing, and testing of microfluidic diodes to increase diodicity - the ratio of 'allowed' to 'obstructed' fluid flow through the diode. The multi-jet modeling (MJM) printer used in this experiment, the Stratasys Objet500 Connex3, allowed the simultaneous printing of both flexible TangoBlack FLX973 and rigid VeroClear RGD810 materials. Its multi-material capabilities allow for dynamic parts that can deform and adjust with fluid flow. Our diode designs were printed in a 10 mm $\times$ 10 mm area with a minimum wall thickness of 3 mm and a tolerance of at least 0.5 mm. Our given experimental testing explored key factors to maximize diodicity, and investigate common modes of failure in the design and manufacturing processes.

2 Design Methods

2.1 Plug Valve

Our plug valve diode (**Fig. 1A**) utilized a single degree of freedom plunger that theoretically would shift inside the diode according to the direction of flow. The streamlined design of the diode would encourage directional flow, while the water would either navigate around the plug in forward flow or build pressure in reverse flow.

2.2 Perforated Valve

The perforated valve design (**Fig. 1C**) utilized a similar single degree of freedom 'plug' but theoretically would allow flow in the forward direction through perforations on the end of the plug. The concept only required a single material to print.

2.3 Plunger Valve

The plunger valve was inspired by the piston-like valve found in the inner workings of a combustion engine. In a car, this design is intended to prevent backflow with gravity assistance. Though the effects of gravity are negligible at the microfluidic scale, we believed the general concept of the oscillating plunger shape would succeed in our experimental testing. This particular design had the smallest features of our six designs. The plunger element was printed in TangoBlack FLX973 and the rest of the diode body was printed in VeroClear RGD810 (Stratasys, Ltd.). **Fig. 1E** shows a cross-sectional rendering of the plunger diode design with the female ports attached to each side.

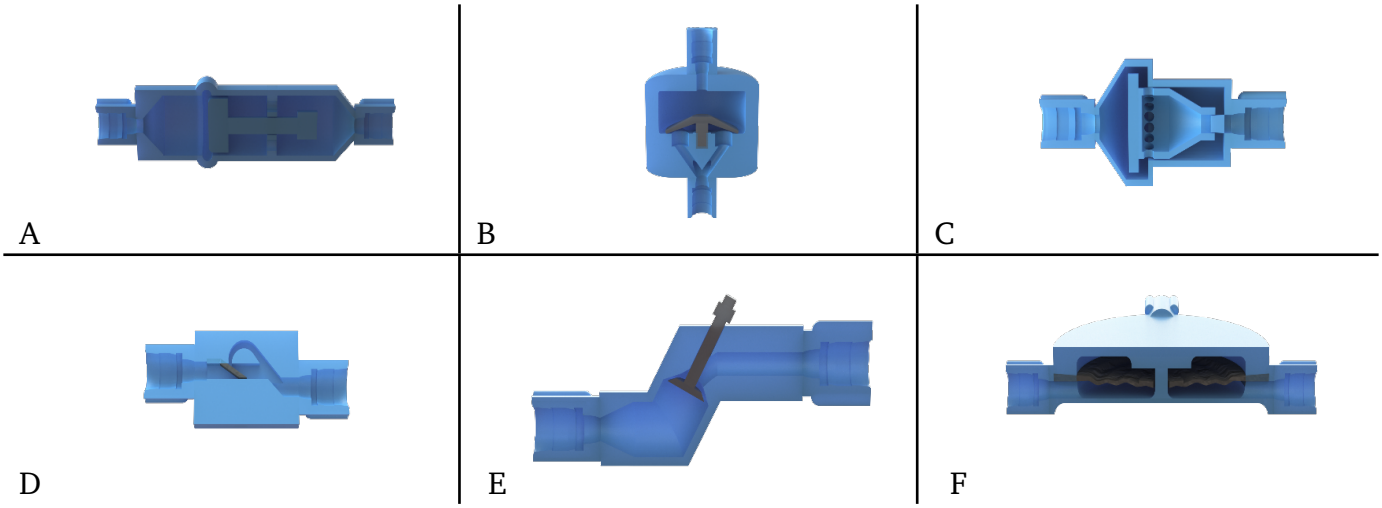

Fig. 1 Renderings of mesofluidic diodes using SolidWorks PhotoView. (A) Plug valve, (B) Umbrella valve, (C) Perforated valve, (D) Tesla Flap valve, (E) Plunger Flap valve, (F) Sochol valve.

2.4 Umbrella Valve

Umbrella diode design was inspired by a small valve manufacturing company, Minivalve. Minivalve, founded in 1999 by Peter Nijland, develops and distributes miniature self-actuating valves, predominantly one way valves, like the umbrella valve. For the umbrella diode (**Fig. 1B**) , the umbrella component was formed with TangoBlack FLX973, a rubber-like material, while the housing component was formed from VeroClear RGD810, a multipurpose transparent plastic. The umbrella concept allows for the material properties and geometry, particularly the thickness, of the umbrella component to dictate the working pressure of the diode. In forward flow conditions, the umbrella's diaphragm like flap acts as a spring sealing the inlet flow until a minimum pressure is reached. When reached, the umbrella is forced into a convex shape, allowing water to pass. In backflow conditions the umbrella's diaphragm like flap is encouraged by the flow to reseal the previous inlet, preventing any flow movement.[7]

2.5 Tesla Flap Valve

Microfluidic diodes have been successfully implemented with both Tesla structures[3,5] and flap-valve mechanisms[6]. This design (**Fig. 1D**) explores potential synergistic effects of these structures to improve diodicity. The flap structure is based upon a mechanical effect in which a TangoBlack FLX973 flap seals to a channel in one direction and opens in the flow direction.[6] The flap forms a 30° nozzle to increase pressure at the bottom of the flap, thereby maximizing flow-driven displacement. The Tesla valve structure has a Y-shaped channel that converges perpendicular to the main channel in reverse flow. In forward flow, the majority of the fluid flows across the main channel with minimal resistance. However, with low Reynold number flows, as typically found in micro/nanofluidics, a flap-less Tesla valve has a low characteristic diodicity $1<Di<2$.[5]

2.6 Sochol Valve

The design for the diode in **Fig. 1F** is based upon a 3D-printed membrane valve developed by Dr. Ryan Sochol. The diode is composed of a peripherally fixed TangoBlack FLX973 annulus separating each side of the diode. In reverse flow, the fluidic pressure across the annulus causes it to deflect, until a flattened section seals across the upper internal surface. In the forward direction, the same pressure driven defection occurs, however, there is no available surface for the annulus to seal against, thereby allowing flow. There is still significant leakage along the central column at the interface between the annulus and housing. The valve presented be Sochol had a uniform material composition, and achieved a diodicity of 80.6.[1] The multimaterial additive manufacturing method allows usage of the TangoBlack FLX973 material, which has superior sealing properties between solid interfaces.

2.7 Numerical Simulation of Stokes Equation

We conducted a flow simulation study in Mathmatica 11 (Wolfram Research Inc., Champaign, Illinois) by evaluating the Stokes equation with limitation of low Reynold's Number. We specified an inflow velocity based upon input flow rate and pressure from the Fluigent system. The outflow pressure was set to zero since we operated the diodes in an atmospheric environment. The fluid velocities are interpolated with second order, while the fluid pressure is interpolated with first order to stabilize the numerical solution. The numerical solutions in **Fig. 2 A,B,C** depict the diodes in forward flow with the flexural members deflected. The solutions in **Fig. 2 D,E,F** present the diodes in reverse flow with the TangoBlack FLX973 interfaces sealing against the VeroClear surfaces.

3 Testing Methods & Results

The diodes were designed with two, standardized female ports at their input and output. A small, clear tube running from a reser-

voir of water in the Fluigent apparatus was inserted into the input port. Another length of clear tube was connected from the output port to a small beaker to collect the outlet fluid. The Fluigent apparatus drives the fluid with pressure, and incrementally records the flow rate through the diode. The resistance of the tubing and the fluidic diodes were calculated at each respective pressure:

$$\Delta P = R_{\text{tot}} \times q_{\text{fluid}}$$

$$\Delta P = (R_{\text{tube}} \times R_{\text{diode}}) \times q_{\text{fluid}}$$

$$R_{\text{total}} = R_{\text{tube}} \times R_{\text{diode}}$$

where R_{total} is the sum of the tube resistance at that pressure (control value) and the resistance of the diode design. Diodicity is the ratio of the resistance to reverse flow over the resistance to forward flow, with resistance being a function of the pressure and flow rate at each increment. The tables and graphs provided in the discussion of testing results are all functions of these equations.

3.1 Plug Valve

The valve revealed design flaws during the testing period that resulted in design failure. **Fig. 1A** includes a rendering of the diode that can reveal the locations for our modes of failure. The manufacturing process consistently printed cracks along the shell of the valve that leaked during testing. The inner cavity section along the plug was never fully removed of support material due to its relatively inaccessible design. Consistent fracturing across the diode prevented flow in either direction.

3.2 Perforated Valve

The testing process revealed the limitations of this design (**Fig. 1C**) as its excessive cavity space and thin-wall structure consistently began to fail. The post-processing support material bath failed to remove all of the material due to our valves design and inadequate time in the bath. The testing process also revealed how the outer wall on the left side of the valve was too thin, and consistently failed. The valve structurally failed during or before diodicity testing occurred.

3.3 Plunger Valve

The plunger valve (**Fig. 1E**) did not experience structural failures or breakage in testing, however it did not display desirable diodicity. Though its small size and cavity shape helped encourage the total removal of support material, it experimentally performed as if it was a straight tube. The tested diodes displayed a diodicity of approximately 1 on each test.

Table 1 Plunger valve diodicity over selective pressure range.

Pressure (mbar)	Forward Flow Rate (μL/min)	Reverse Flow Rate (μL/ min)	Diodicity
50	230	225	1.049
100	440	400	1.212
150	560	555	1.016

3.4 Umbrella Valve

The umbrella valve (**Fig. 1B**) was one of three designs that we considered successful in realizing design objectives for the project. Initially displaying infinite resistance for both forward and back flow conditions, the design eventually became fully functional at higher pressures. Its large cavity size, in relation to the size of the inlet and outlet, contributed to the lack of support removal and its initial dysfunction. Experimentally, it performed as expected only at higher pressures. **Table 2** is a synopsis of the performance of the three valves that had the most support material removed to allow functionality. They display an average diodicity of approximately 80, meaning successful additional impedance in backflow conditions compared to forward flow.

Table 2 Umbrella valve diodicty over selective pressure range.

Pressure (mbar)	Forward Flow Rate (μL/min)	Reverse Flow Rate (μL/ min)	Diodicity
100	0	0	N/A
150	0	0	N/A
2000	690	10	74.92
3000	820	10	86.04

3.5 Tesla Flap

The sealing mechanism performed as intended under low pressures, though at a pressure of 200 mbar, the diode failed and became inoperable. Due to the small wall thickness of the flap, the high force caused complete mechanical failure at the fixed portion of the flap. Prior to mechanical failure, this diode resulted in an average diodicity of 885 over the tested range. The diodicity appears to inversely relate with forward flow rate.

Table 3 Tesla Flap valve diodicity over selective pressure range.

Pressure (mbar)	Forward Flow Rate (μL/min)	Reverse Flow Rate (μL/ min)	Diodicity
50	350	1	2208
100	300	1.5	312
150	650	10	135
200	N/A	N/A	N/A

3.6 Sochol Valve

The multi-material modification to this valve enhanced the diodicity by 275% to an average diodicity of 222.

Table 4 Sochol valve diodicity over selective pressure range.

Pressure (mbar)	Forward Flow Rate (μL/min)	Reverse Flow Rate (μL/ min)	Diodicity
100	200	1	384
150	240	2	168
2000	495	7	117
3000	350	2	221

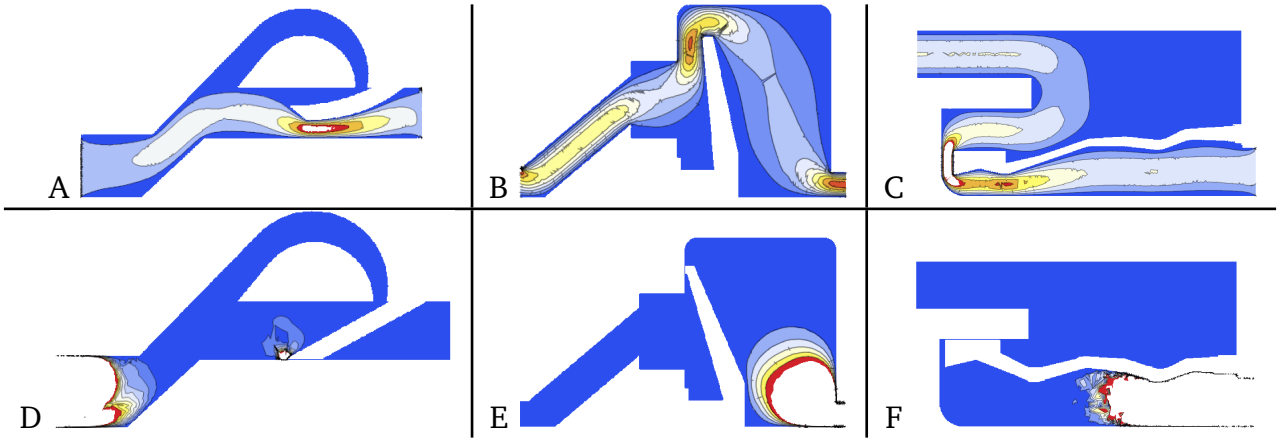

Fig. 2 Fluid flow simulations of functioning mesofluic diodes. Tesla Flap, Umbrella, and Sochol diodes in open configuration (A,B,C) and closed (D,E,F) respectively.

Fig. 3 Diodicity with Reynold's number. (d = inlet diameter)

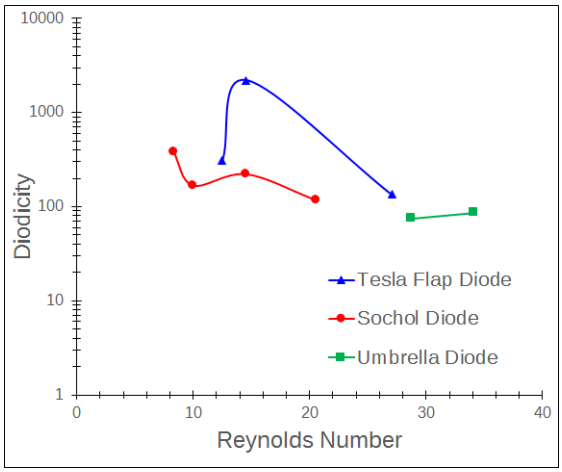

4 Conclusions

After exploring the benefits of MJM based design, as it relates to meso fluidic diodes, several conclusions can be drawn about the design process, experimental results, and expected future work. The experimental results show exceptional diodicities for the Tesla Flap, Sochol, and Umbrella valves, but the limited number of test trials, and data, obscure the consistency and validity of the performance of each diode. More trials and research into the designs must be done to further validate experimental results. Validation of the calculated tube resistance, used to find the diodicity, should also be done due to inconsistent experimental procedures and our lack of tube length data. This discrepancy could result in diodicity ratios that are lower than reality.

The multi-material aspect of MJM based design contributed to the success of actuating diodes. This variance in material allowed for design flexibility centered around the material's properties. These properties combined with tolerancing, specifically in the umbrella diode and the tesla flap, were key to its' performance. A balance must be reached between the designed thickness of the rubber component and their withstanding of the post processing involved with MJM. If this part is designed too thin you risk damaging the rubber via erosion during soluble support removal. If designed too thick you increase the minimum working pressure for the diode. For the umbrella valve, for example, we designed too thick. As seen in the experimental results, the working pressure is ten time that of other diode designs.

A relationship between the successful removal of support material and relative size of the inlet/outlet cross section to diode cross section was found during experimentation. The Tesla Flap, Sochol, and plunger valves had support removed successfully, while the umbrella, perforated, and plunger valves remained filled with support. The distinction between the three suggest that the ratio of the inlet and outlet cross section to the diode cross section must be less than or equal to one, or close to one. Ratios that are too large increase the volume of support material within the diode, while maintaining the same access constraint, the inlet/outlet cross section. More research must be done to establish an explicit relationship between the inlet/outlet cross section to the inner feature cross section of MJM printed devices; and the effects these parameters have on the rate of mass transfer during support removal. It is also worth noting that our designs shared the solvent solution with another group of parts that had an excessive amount of support material in and around the diodes. This diluted the chemical mix and undoubtedly made the removal process move slower.

5 Acknowledgements

Special thanks to Dr. Sochol for his engaging lectures and commitment to his students, to Yanbin for his time and effort making sure our designs printed successfully, to Parth Desai for his help in class and in the lab, and to Terrapin Works for handling our print submissions for this project. All renderings were completed in SolidWorks and simulations were executed in Mathematica.

References

1 R. D. Sochol, E. Sweet, C. C. Glick, S. Venkatesh, A. Avetisyan, K. F. Ekman, A. Raulinaitis, A. Tsai, A. Wienkers, K. Korner, K. Hanson, A. Long, B. J. Hightower, G. Slatton, D. C. Burnett,

T. L. Massey, K. Iwai, L. P. Lee, K. S. J. Pister and L. Lin, *Lab Chip*, 2016, **16**, 668–678.

2 A. J. Morgan, L. Hidalgo San Jose, W. D. Jamieson, J. M. Wymant, B. Song, P. Stephens, D. A. Barrow and O. K. Castell, *PLoS ONE*, 2016, **11**, e0152023.

3 N. Tesla, *Valvular conduit*, 1920, https://www.google.com/patents/US1329559, US Patent 1,329,559.

4 S. Ragan, *The Tesla Valve: One Way Flow With No Moving Parts | Make:*, 2012, http://makezine.com/2012/01/05/the-tesla-valve-one-way-flow-with-no-moving-parts/.

5 K. F. Forester, *Journal of Fluids Engineering*, 2002, **82**, 431–437.

6 M. L. Adams, M. L. Johnston, A. Scherer and S. R. Quake, *Journal of Micromechanics and Microengineering*, 2005, **15**, 1517.

7 M. Inc., *Umbrella Valves, Belleville Valves, How they work! (patent pending)*, http://www.minivalve.com/newsite/index.php/en/by-type/umbrella-valves/how-they-work.